



Effects of trophic status, water level, and temperature on shallow lake metabolism and metabolic balance: A standardized pan-European mesocosm experiment

Ulrike Scharfenberger ^{1,2*} Erik Jeppesen,^{3,4} Meryem Beklioglu,^{5,6} Martin Søndergaard,³ David G. Angeler,⁷ Ayşe İdil Çakiroğlu,⁸ Stina Drakare,⁷ Josef Hejzlar,⁹ Aldoushy Mahdy,¹⁰ Eva Papastergiadou,¹¹ Michal Šorf,^{9,12} Konstantinos Stefanidis,¹³ Arvo Tuvikene,¹⁴ Priit Zingel ¹⁴, Rita Adrian^{1,2}

¹Department of Ecosystem Research, Leibniz Institute of Freshwater Ecology and Inland Fisheries (IGB), Berlin, Germany

²Department of Biology, Chemistry, and Pharmacy, Freie Universität Berlin, Berlin, Germany

³Department of Bioscience and the Arctic Research Centre, Aarhus University, Silkeborg, Denmark

⁴Sino-Danish Centre for Education and Research (SDC), Beijing, China

⁵Department of Biology, Limnology Laboratory, Üniversiteler Mahallesi, Middle East Technical University, Çankaya, Ankara, Turkey

⁶Kemal Kurdas, Ecological Research and Training Station, Lake Eymir, Middle East Technical University, Çankaya, Ankara, Turkey

⁷Department of Aquatic Sciences and Assessment, Swedish University of Agricultural Sciences, Uppsala, Sweden

⁸Mechanical Engineering Department, Koc University, Sarıyer, Istanbul, Turkey

⁹Biology Centre of the Czech Academy of Sciences, Institute of Hydrobiology, České Budějovice, Czech Republic

¹⁰Department of Zoology, Faculty of Science, Al-Azhar University (Assiut Branch), Assiut, Egypt

¹¹Department of Biology, University of Patras, Rio, Greece

¹²Faculty of Science, University of South Bohemia, České Budějovice, Czech Republic

¹³Department of Water Resources and Environmental Engineering, School of Civil Engineering, National Technical University of Athens, Athens, Greece

¹⁴Centre for Limnology, Institute of Agricultural and Environmental Sciences, Estonian University of Life Sciences, Tartumaa, Estonia

Abstract

Important drivers of gross primary production (GPP) and ecosystem respiration (ER) in lakes are temperature, nutrients, and light availability, which are predicted to be affected by climate change. Little is known about how these three factors jointly influence shallow lakes metabolism and metabolic status as net heterotrophic or autotrophic. We conducted a pan-European standardized mesocosm experiment covering a temperature gradient from Sweden to Greece to test the differential temperature sensitivity of GPP and ER at two nutrient levels (mesotrophic or eutrophic) crossed with two water levels (1 m and 2 m) to simulate different light regimes. The findings from our experiment were compared with predictions made according the metabolic theory of ecology (MTE). GPP and ER were significantly higher in eutrophic mesocosms than in mesotrophic ones, and in shallow mesocosms compared to deep ones, while nutrient status and depth did not interact. The estimated temperature gains for ER of ~ 0.62 eV were comparable with those predicted by MTE. Temperature sensitivity for GPP was slightly higher than expected ~ 0.54 eV, but when corrected for daylight length, it was more consistent with predictions from MTE ~ 0.31 eV. The threshold temperature for the switch from autotrophy to heterotrophy was lower under mesotrophic (~ 11°C) than eutrophic conditions (~ 20°C). Therefore, despite a lack of significant temperature-treatment interactions in driving metabolism, the mesocosm's nutrient level proved to be crucial for how much warming a system can tolerate before it switches from net autotrophy to net heterotrophy.

The balance between gross primary production (GPP) and ecosystem respiration (ER) determines the metabolic status of

lakes and has a decisive influence on their role in regional/global matter and energy cycles (Andersson and Sobek 2006; Brothers et al. 2013; Pacheco et al. 2014). Shallow lakes are the most numerous lake type on Earth (Cael et al. 2017), and have been recognized as hotspots of carbon turnover (Cole et al. 2007; Tranvik et al. 2009). While oligotrophic lakes with

*Correspondence: scharfenberger@igb-berlin.de

Additional Supporting Information may be found in the online version of this article.

high-allochthonous carbon inputs tend to be predominantly net heterotrophic ($GPP < ER$), many eutrophied lakes have been found to be net autotrophic ($GPP > ER$) (del Giorgio and Peters 1994; Cole et al. 2000; Balmer and Downing 2011). Lakes can switch between net autotrophy and net heterotrophy across multiple timescales (i.e., daily, weekly, or seasonal) (Staehr and Sand-Jensen 2007; Coloso et al. 2011; Sadro et al. 2011; Laas et al. 2012); in temperate lakes, the extent of net autotrophy in spring and summer can be a determining factor for the annual metabolic status of lakes (Staehr et al. 2010; Laas et al. 2012). Autotrophic and heterotrophic metabolic pathways are susceptible to changes in light regime, nutrient status, and temperature. All these drivers are predicted to be affected by climate change due to alterations in water levels, nutrient cycling, and run-off from the catchment (Coops et al. 2003; Nickus et al. 2010; Jeppesen et al. 2015).

The metabolic theory of ecology (MTE) provides a comprehensive theoretical framework to investigate metabolic rates' dependence on temperature (Brown et al. 2004). Based on first principles, the MTE allows the scaling of metabolic rates from individual biochemical reactions up to the level of ecosystems (Enquist et al. 2003; Allen et al. 2005; Yvon-Durocher et al. 2010b). Independent of temperature, the absolute metabolic rate at the ecosystem level is primarily determined by the size and abundance distribution of the constituting community of the ecosystem. On the other hand, the physiological dependence of metabolic rates on temperature, approximated by the Arrhenius equation, is still governed by the rate-limiting biochemical process of the cellular level, even at the ecosystem level (Bernacchi et al. 2001; Gillooly et al. 2001; Allen et al. 2005). Under nonlimiting conditions, the MTE assumes activation energies of ≈ 0.3 eV (photosynthesis) and ≈ 0.6 eV (respiration). Therefore, in a warming world, the MTE predicts a shift toward heterotrophy (as temperatures increase) or even a switch from net autotrophy to net heterotrophy if stored or allochthonous carbon sources are available (Yvon-Durocher et al. 2010a; Laas et al. 2012; Weyhenmeyer et al. 2015). A shift toward heterotrophy would imply a reduction in the carbon sequestration capacity or even loss of this important ecosystem service as a carbon sink, unless offset by sedimentation rates. The temperature at which a net autotrophic system switches to net heterotrophy depends, however, not only on the differential temperature sensitivity of GPP and ER, but also on the ratio of the absolute GPP and ER rates. Theoretically, the more GPP exceeds ER at a given reference temperature, the more warming a lake can tolerate before switching from net autotrophy to net heterotrophy.

Since temperature and eutrophication are regarded as the two major stressors for lake ecosystems, several studies have documented their effects on GPP, ER, and the balance between them. Several of these studies have confirmed the occurrence of positive effects of temperature on both ER and GPP, but negative effects on net ecosystem production

($NEP = GPP - ER$) (Kosten et al. 2010; Moss 2010; Yvon-Durocher et al. 2010a,b, 2012). Moreover, there is general agreement that elevated nutrient concentrations promote metabolic rates, but have greater impact on GPP than ER, causing increases in NEP, or decreases in ER/GPP ratios (del Giorgio and Peters 1994; Hanson et al. 2003; Duarte et al. 2004; Staehr et al. 2010) as well as a stronger coupling between ER and GPP in oligotrophic than in eutrophic lakes (Solomon et al. 2013). However, the interacting effects of temperature and trophic state on ecosystem metabolism within the context of already observed and predicted changes in lake water levels, and thus light conditions, are not well understood (Anderson-Teixeira and Vitousek 2012; Cross et al. 2015; Welter et al. 2015), and results from experiments on nutrient-temperature interactions are ambiguous (Berggren et al. 2010; Moss 2010; Liboriussen et al. 2011).

In particular, it is unclear how interactions between temperature, nutrients, and light availability can modify the MTE predicted values for the activation energy resulting in deviations of the apparent temperature sensitivity at ecosystem level from the physiological one (Cross et al. 2015), thereby modifying the MTE-predicted shift toward heterotrophy with increasing temperature. Models combining Arrhenius and Michaelis-Menten kinetics have shown, for instance, that substrate limitation and trophic structure can dampen the apparent temperature sensitivity (Davidson et al. 2012, 2015). In addition, both the maximum rate and the half-saturation constant were found to increase with increasing temperature in photosynthesis-irradiance relations (Kirk 2010). However, temperature-dependent increases in the photosynthetic rate might be subdued if phosphorus limits the process (Wykoff et al. 1998; Kirk 2010). In accordance with this, Staehr and Sand-Jensen (2006) found a reduced metabolic response in a natural algae assembly to increased temperatures under nutrient-limiting conditions. Reduced light and nutrient conditions may affect ER either due to substrate limitation or changes in food quality (McFeeters and Frost 2011). However, results from laboratory experiments are difficult to scale to the ecosystem level, where covariation of temperature with factors such as water level, daylight length, nutrient cycling, and N_2 fixation, as well as acclimation and adaptation at species or community levels can all influence the apparent temperature sensitivity (Atkin and Tjoelker 2003; Anderson-Teixeira and Vitousek 2012; Welter et al. 2015).

Based on a standardized pan-European mesocosm experiment, this study aims to improve the understanding of how the combined effects of water temperature, water level, and nutrient status affect metabolic rates in shallow lake ecosystems. Specifically, we investigated temperature effects on GPP, ER, and the ratio of ER/GPP under eutrophic and mesotrophic nutrient conditions and at two depth levels, simulating different light conditions. The findings from our experiment were compared with predictions made according to the theoretical framework of the MTE. We tested the following hypotheses:

(1) Metabolic rates are lower with reduced nutrient availability, but increase at lower water levels due to higher light availability; (2) a shift toward heterotrophy occurs with increasing temperature due to a higher physiological temperature sensitivity of ER compared with GPP; (3) the apparent temperature sensitivity of ER and GPP will differ between treatments due to interactions between temperature, the availability of light, and nutrients; (4) switching between auto- and heterotrophy occur at lower temperatures if the magnitude of ER and GPP is more similar (NEP near zero). We expect this situation under low-nutrient and low-light conditions that sustain a generally lower lake GPP.

Materials and methods

Experimental design and sampling

The mesocosm experiment was conducted in six European countries, encompassing a climate gradient from Sweden to Greece (Table 1) from May 2011 until November 2011. The fiberglass mesocosms used were produced by the same manufacturer, and had a diameter of 1.2 m and heights of 1.2 m or 2.2 m. The mesocosms were set up within the lakes to ensure a natural and ambient water temperature regime, but were otherwise isolated from the surrounding water. In each country, the experiment involved a 2 × 2 factorial design with four replicates; measurements were taken monthly. The first factor involved two different water levels: 1 m (shallow-S) and 2 m (deep-D) deep mesocosms. These two depths coincided with different mixing depths, since the water in the mesocosms was constantly circulated from bottom to top by standard aquarium pumps, entailing different light conditions (Supporting Information S3 Fig. 1). Water levels were allowed to fluctuate with precipitation and evaporation. The second factor involved nutrient manipulation to simulate mesotrophic (low-L) and eutrophic (high-H) conditions. Nutrients were adjusted to the

two conditions by monthly nutrient addition aiming at initial concentrations after loading of 25 μg phosphate (P) L^{-1} (Na_2HPO_4) and 0.5 mg nitrogen (N) L^{-1} ($\text{Ca}(\text{NO}_3)_2$) in the mesotrophic and 200 μg P L^{-1} and 2 mg N L^{-1} in the eutrophic treatment. The experiment was synchronized using a common protocol to facilitate comparability (Landkildehus et al. 2014).

The mesocosms contained a 10 cm sediment layer of 90% washed sand and 10% natural sediment from an oligotrophic lake, situated near the respective experimental site. To prevent prolonged internal P loading (low-nutrient conditions) or P retention (high-nutrient conditions) at the start of the experiment, the sediment was acclimatized to the desired phosphate concentrations for at least 2 months in the laboratory beforehand. Filtered (500 μm mesh) lake water was used in the mesocosms in all countries except Germany and the Czech Republic, where tap water was used because the P level exceeded the 25 μg TP L^{-1} threshold of the low-nutrient treatment. The initial P and N loadings were adjusted in all high-nutrient mesocosms to obtain the desired nutrient concentration.

The ability of natural flora and fauna to adapt to the specific climate and nutrient conditions was ensured by using an inoculum of plankton and sediment collected from five different local lakes, covering a nutrient gradient from 25 μg TP L^{-1} to 200 μg TP L^{-1} in each country. Macrophytes (*Myriophyllum spicatum*) and planktivorous fish were added to all mesocosms. Monthly samples were analyzed for water chemistry and chlorophyll *a* (Chl *a*) in laboratories and on site by using comparable, standard methods (see Supporting Information S2 Table 1). Concomitantly, macrophyte biomass was quantified as plant volume inhabited (PVI [%]). After each sampling event, 24-h measurement of dissolved oxygen and water temperature was conducted at 2-h intervals using a multiparameter probe (for sampling dates, see Supporting Information S1 Table 1). In addition, light profiles of the water column

Table 1. Location of experimental sites and average temperatures. Average air temperatures were calculated based on daily average air temperatures of the periods leading up to the 24-h measurements as defined in Supporting Information S1 Table 1. Water temperatures are daily averages based on 24-h point measurements (Supporting Information S1 Table 1).

Experimental site	Coordinates	Altitude (m a.s.l.)	Air temperature (°C)			Water temperature (°C)		
			Mean	Min	Max	Mean	Min	Max
Sweden (SE)—Erken	59°49'59"N 18°33'55"E	11	14.5	8.7	18.8	14.9	8.1	22.0
Estonia (EE)—Võrtsjärv	58°12'17"N 26°06'16"E	35	15.1	7.5	19.9	16.3	6.8	24.0
Germany (GE)—Müggelsee	52°26'0"N 13°39'0"E	32	16.0	9.6	18.4	17.7	9.7	21.7
Czech Republic (CZ)—Vodňany	49°09'14"N 14°10'11"E	395	15.2	7.5	18.8	16.0	8.1	22.0
Turkey (TR)—ODTÜ-DSİ Gölet	39°52'38"N 32°46'32"E	998	20.0	10.4	26.2	19.3	8.2	25.6
Greece (GR)—Lysimachia	38°33'40"N 21°22'10"E	16	23.8	15.0	27.9	24.8	15.4	29.1

were measured at midday at 10 cm intervals. For details on the design and sampling, see Landkildehus et al. (2014).

Data preparation

The study utilized the data collected between July and November, under the assumption that all systems would have had enough time to adjust to the experimental manipulation by then. Seven mesocosms were excluded from the analysis (2 deep high nutrient [DH], 1 deep low nutrient [DL], and 1 shallow high nutrient [SH] mesocosm in Germany and 2 SH and 1 shallow low nutrient [SL] mesocosm in the Czech Republic) as they were lost during storm events. The analysis is thus based on five measurements, including data from 89 mesocosms per measurement occasion. In Greece, massive water loss due to evaporation prevented sampling in the shallow mesocosms, involving light profiles (from September onward), water chemistry (from October onward), and the 24-h measurement in November. Since visual inspection of these shallow mesocosms indicated high light attenuation, we assumed the same high attenuation for the remaining sampling occasions. Light profiles were also missing for August and September for the Estonian mesocosms. Here, the missing attenuation coefficients were linearly interpolated since none of the attenuation coefficients from the other countries indicated strong seasonality.

All data were visually inspected at the raw data level and outliers were identified using boxplots. Only extreme outliers (larger than three times the interquartile range) were removed from the data (O_2 : 36 values [1%] and water temperature: 4 values [0.1%]) and replaced by interpolated values. Single gaps in the 24-h data were substituted by values from a polynomial model of degree 4 of time; for all other data linear interpolation were used. Reported average values (e.g., average air temperature) correspond to the sampling periods listed in Supporting Information S1 Table 1.

Estimation of reaeration coefficient ($K_{a,20}$ [h^{-1}]) at 20°C for O_2

To ensure minimal influence from respiration, gas exchange was measured when water temperatures were low and after the last sampling in late October, or early November. Under continuous mixing, oxygen saturation was lowered to approximately 30% by bubbling N_2 into two randomly chosen shallow and deep mesocosms. At nightfall, oxygen reduction was completed and oxygen recovery was monitored overnight (reaeration). For each mesocosm, a transport coefficient $K_{L,20}$ was estimated following Liboriussen et al. (2011). Two different respiration models were tested: $R_{20^\circ C} 1.047^{(T-20)}$ (Erlandsen and Thyseen 1983) and $R_{20^\circ C} 1.07^{(T-20)}$ (Streeter and Phelps 1925; De Matos et al. 2014). The model outputs did not differ systematically and differences were generally low. Since both models are plausible representations of the temperature effect on respiration, we synthesized the results into an average $K_{L,20}$ value (0.0218 $m h^{-1}$). However, values

from the Czech mesocosms were excluded because the O_2 reductions were too low to permit proper calculations. Averaging was chosen to appropriately reflect modeling uncertainty, which is in line with the idea of ensemble modeling. $K_{a,20}$ values were then derived by dividing by the mixing depth.

Estimation of GPP and ER

Metabolic rates were estimated based on the 24-h O_2 measurements using the free-water method following Jeppesen et al. (2012). Since the main focus of the investigation was to analyze the temperature response of the metabolic rate, Arrhenius-type corrections based on a priori Q10 values from the literature were avoided.

To assess the uncertainty of the estimated metabolic rates, we used a bootstrap approach similar to the one described in Solomon et al. (2013). Estimates with standard errors larger than the estimate itself, and estimates explaining < 5% of the variability of the 24-h dissolved oxygen curve, were excluded from further analysis, totaling 14% of the values. Overall, 374 data points remained. For an overview of the distribution of data points per country, month, and treatment, see Supporting Information S1 Table 2. To obtain daylight length-corrected GPP values, GPP_{dl} [$mg m^{-3} hd^{-1}$], GPP per day was divided by the average daylight period, LP (hd^{-1}), according to month and country. For further details on the estimation of metabolic rates and the meteorological data used, see Supporting Information S2.

Estimation of light attenuation coefficient (K_d), mean available light, and effective light period

For each light profile, an attenuation coefficient (K_d) was estimated based on the Beer-Lambert law. Mean available light (MAL) over the water column was estimated following Staehr et al. (2010). The effective light period (LP_{eff}), describing the effective light period due to mixing, was calculated following Shatwell et al. (2012). For more details, see Supporting Information S2.

Hypotheses generation based on MTE

We used the framework of the MTE to formally derive the expected temperature dependence of the measured metabolic rates and the ratio between them, which we tested against our experimental findings. Following the MTE, the temperature dependence of metabolic rates can be approximated by the Arrhenius equation within a temperature range of 0–30°C (Gillooly et al. 2001; Brown et al. 2004; Allen et al. 2005). At the ecosystem level, the MTE is formulated as:

$$M(T) = M_0 \exp\left(\frac{-E}{kT}\right) \quad (1)$$

where $M(T)$ is the temperature-dependent metabolic rate; M_0 at the ecosystem level can be interpreted as the size-dependent basic metabolic flux summed over all autotrophs or heterotrophs,

respectively, per unit volume (Allen et al. 2005); E is the activation energy and expresses the strength of the temperature effect on the metabolic rate; k is the Boltzmann constant ($8.62 \times 10^{-5} \text{ eVK}^{-1}$); and T is the absolute temperature in Kelvin. The above temperature effect can be conveniently analyzed and plotted with Arrhenius plots based on the logarithmized version of Eq. 1. In Arrhenius plots, the natural logarithm of the metabolic rate is plotted against the inverse and scaled temperature $1/(kT)$ so that the slope of this linear relationship represents the activation energy and the intercept the absolute metabolic rate of a particular metabolic process. The absolute metabolic rate is usually shifted to a biological meaningful reference temperature (T_c), here to 15°C , following Yvon-Durocher et al. (2010b) and Demars et al. (2011). Thus, the MTE equation used to analyze the temperature dependence of metabolic rates reads:

$$\ln M(T) = \ln M_{T_c} + E \frac{1}{k} \left(\frac{1}{T_c} - \frac{1}{T} \right) \quad (2)$$

At the ecosystem level, resource availability could either affect the absolute metabolic rate or the apparent activation energy, E .

To derive the expected temperature effects for the ER/GPP ratio, we assumed, following Yvon-Durocher et al. (2010b), that our systems were in a nonsteady state and that ER is mainly driven by heterotrophic metabolism, unconstrained by net primary production (for data-driven justification of the assumption, see Supporting Information S6). Thus, the temperature-driven change of the ratio between ER and GPP can be simplified to:

$$\frac{\text{ER}}{\text{GPP}}(T) = \frac{\text{ER}_0}{\text{GPP}_0} \exp\left(\frac{E_p - E_r}{kT}\right) \quad (3)$$

where $\text{ER}/\text{GPP}(T)$ is the temperature-dependent metabolic ratio; ER_0 and GPP_0 are the absolute metabolic rates according to the definition of M_0 ; and E_p and E_r are the activation energies for GPP and ER, respectively.

Again, the Arrhenius plot together with a shift to a biological meaningful reference temperature can be used to analyze and depict the relationship in logarithmic terms:

$$\ln \frac{\text{ER}}{\text{GPP}}(T) = \ln \frac{\text{ER}_{T_c}}{\text{GPP}_{T_c}} - \frac{E_p - E_r}{k} \left(\frac{1}{T_c} - \frac{1}{T} \right) \quad (4)$$

where GPP_{T_c} and ER_{T_c} are the GPP and ER rate at the reference temperature, T_c ; and E_p and E_r are the activation energies for GPP and ER, respectively. Equations 2, 4 explicitly state that changes in the metabolic balance with changing temperature, and thus its influence on the carbon sequestration capacity, depend solely on the amount of differential temperature sensitivity between ER and GPP.

Based on the MTE, we derived an expectation about the temperature at which the switch from autotrophy to

heterotrophy occurs. Formally, this is the point of equality between GPP and ER, given by:

$$T = \frac{1}{\frac{k \ln \frac{\text{GPP}_{T_c}}{\text{ER}_{T_c}}}{E_p - E_r} + \frac{1}{T_c}} \quad (5)$$

For fixed E_p and E_r , the switch point depends solely on the ratio between GPP_{T_c} and ER_{T_c} , i.e., the smaller the ER_{T_c} relative to GPP_{T_c} , the higher the temperature at which the system switches from autotrophy to heterotrophy. Thus, assuming resource-dependent absolute $\text{ER}_{T_c}/\text{GPP}_{T_c}$ values, the switch point from autotrophy to heterotrophy should be lower in light- and nutrient-reduced environments.

Statistical analysis

All statistical analyses were conducted using R version 3.1.3 (R Core Team 2015). We analyzed temperature and treatment effects based on monthly data from all countries using linear mixed effect models (“lme4” package, Bates et al. 2014). The following basic model was applied:

$$\ln M_{c,(s,m),i}^{(D \times N)}(T) = \overline{\ln M_{T_c}^{(D \times N)}} + \epsilon_R^c + \epsilon_R^{c,s} + \epsilon_R^{c,m} + \left(\overline{E^{(D \times N)}} + \epsilon_E^c + \epsilon_E^{c,m} \right) \frac{1}{k} \left(\frac{1}{T_c} - \frac{1}{T} \right) + \epsilon_{c,(s,m),i} \quad (6)$$

where $\ln M_{c,(s,m),i}^{(D \times N)}$ and $\epsilon_{c,(s,m),i}$ are the temperature-dependent metabolic rate and associated random error for measurement i of mesocosm m in month s and country c ; k is the Boltzmann constant; and T_c is the reference temperature set to 15°C as in Eqs. 2, 4. $\overline{\ln M_{T_c}^{(D \times N)}}$ and $\overline{E^{(D \times N)}}$ are the logarithmic average metabolic rate at T_c , and the average apparent activation energy, respectively, for each treatment. For the average metabolic rate at 15°C , random effects at the level of country (ϵ_R^c), month ($\epsilon_R^{c,s}$), and mesocosm ($\epsilon_R^{c,m}$) were considered, where both month and mesocosm are nested within country. For the average apparent activation energy, random effects on the level of country (ϵ_E^c) and mesocosm ($\epsilon_E^{c,m}$) were taken into account as well. The random effect on the level of mesocosm was nested within country. Following Yvon-Durocher et al. (2012), the random effect of month was added to control for confounding effects on apparent activation energy, which a potential covariation between monthly absolute metabolic rates and temperature may cause. With this modeling approach, we assumed a generic activation energy as suggested by MTE, with an additional possibility of random variation between countries and mesocosms due to interactions and covariation with factors other than those controlled for experimentally. These assumptions are justified, since country-specific activation energies and absolute metabolic rates at 15°C did not reveal systematic changes in relation to average

temperature (Supporting Information S4). In this situation, the mixed-effect models approach that we chose is reliably capable of estimating the average activation energy as well as the absolute metabolic rate, as validated in a simulation approach emulating the structure and random structure of our experimental data (Supporting Information S8).

The same basic model as in Eq. 6 was used for the analysis of GPP, daylight length-corrected GPP_{dl}, ER, and the ER/GPP ratio. Model selection of random and fixed effects was done based on likelihood ratio tests by stepwise backward elimination (“lmerTest” package, Kuznetsova et al. 2014; “step” function). However, we retained the main effects of depth, nutrients, and temperature as a minimum, since we—apart from significance—sought to describe effect size and to conduct comparisons between estimated and predicted values based on the MTE. Effect sizes were calculated using standardized predictors following Gelman (2008). Model validation was conducted by graphical inspection of the Pearson residuals, including their relation to all predictor variables. The model fit was assessed by conditional (variance explained by fixed effects) and marginal (variance explained by fixed and random effects) coefficients of determination (“MuMIn” package, Bartoń 2015; “r.squaredGLMM” function). Treatment-specific confidence intervals were computed based on a “t” statistic with degrees of freedom established by the Kenward-Rogers method (“lsmeans” package, Lenth and Hervé 2015; function “lsmeans”).

Covariation of temperature, depth, and nutrient levels with total phosphorus (TP), total nitrogen (TN), K_d , MAL, LP_{eff}, Chl *a*, and PVI was assessed with the same basic mixed effects model as in Eq. 6. However, rather than the scaled inverse water temperature, a centered water temperature of 15°C was used. Box-Cox transformation was applied for the dependent variable to meet model assumptions (“MASS” package, Ripley

et al. 2015; “boxcox” function). Factor covariate interaction was probed using two-tailed *t*-tests for pairwise comparisons of least-square-means over the temperature gradients at one degree intervals (“lsmeans” package; Lenth and Hervé 2015). Reported treatment-wise adjusted means (“phia” package, De Rosario-Martinez 2015; “InteractionMeans” function) as well as the direction and amount of average change between 7°C and 29°C (the temperature range we tested) were estimated based on these models.

Using semi-partial Spearman correlation, we assessed the differential influence of MAL, LP_{eff}, daylight length, Chl *a*, PVI, and inverse and scaled water temperatures on GPP, ER, and the ER/GPP ratio (“ppcor” package, Kim 2012; “spcor” function). Semi-partial Spearman correlation coefficient *r* and percentile 95% confidence intervals were bootstrapped over mesocosms (“boot” package, Canty and Ripley 2015; “boot” and “boot.ci” function). To further disentangle the influence of daylight lengths from the effect of temperature on GPP, we compared the results from two separate regression models based on standardized variables, conducted a residual regression analysis (see Supporting Information S7), and analyzed daylight length-corrected GPP (Allen et al. 2005).

Results

Water temperatures revealed a distinct seasonal pattern in all countries (Table 1; Fig. 1a). From July 2011 to November 2011, water temperature ranged from 6.8°C to 29.1°C (all countries included). Water temperatures were highly correlated with monthly mean air temperatures ($r = 0.88$ with a 95% confidence interval of 0.85–0.90), confirming that the monthly point measurements in our enclosures represented the overall seasonal temperature conditions (Table 1).

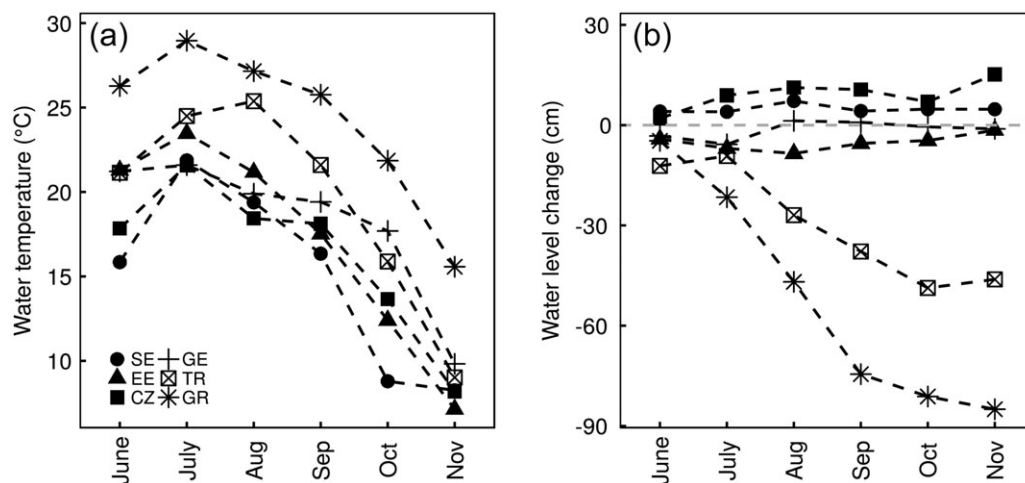


Fig. 1. (a) Development of water temperature and (b) change in water level due to evaporation losses and precipitation gains over the experimental period from June to November by country. SE, Sweden; EE, Estonia; CZ, Czech Republic; GE, Germany; TR, Turkey; GR, Greece.

The water level decreased drastically in the two southern countries during autumn, while changes were modest in the central and northern European countries (Fig. 1b).

The differential monthly loading of phosphate resulted in significantly (< 0.05) different TP levels between the high-nutrient and low-nutrient mesocosms over the entire temperature gradient (Fig. 2a, Supporting Information S3 Table 1). TN levels between deep eutrophic mesocosms and both low-nutrient treatments were not significant for temperatures above $\sim 25^{\circ}\text{C}$ (Fig. 2b, Supporting Information S3 Table 1). Light availability, as measured by the MAL and the effective light period (LP_{eff}), was highest in the shallow mesotrophic followed by the shallow eutrophic mesocosms, and the deep mesotrophic mesocosms; it was lowest in the deep eutrophic mesocosms (Supporting Information S3 Fig. 1b,c). Over the entire temperature gradient, MAL differed significantly (< 0.05) between all treatments (for DL – SH above 9°C). LP_{eff} was significantly shorter in the deep eutrophic mesocosms compared to all other treatments. The deep mesotrophic mesocosm had shorter LP_{eff} compared with the shallow mesocosms for temperatures above 15°C (SL) and 21°C (SH), while at no point did LP_{eff} values differ significantly among the shallow mesocosms (Supporting Information S3 Fig. 1 and S3 Table 1).

Nutrient and light effects on average metabolic rates (Hypothesis 1)

On average, GPP and ER were significantly higher in the eutrophic than in the mesotrophic systems, and significantly higher in the shallow than in the deep mesocosms (Table 2; Fig. 3). In line with our expectations, the eutrophic shallow mesocosms with ample light had the highest metabolic rates, followed by eutrophic deep systems with reduced light availability, shallow mesotrophic systems with ample light, and deep mesotrophic light-reduced systems.

Temperature and interaction effects (Hypotheses 2 and 3)

Both log-transformed GPP and ER increased significantly with increasing temperatures as predicted by the Arrhenius Eqs. 1, 2 (Fig. 4; Table 2). Contrary to our expectations, we found no significant interacting effects between water temperature and the different light and nutrient regimes on GPP and ER. The average temperature sensitivity of ER in all treatments was 0.62, predicting a 13.5-fold increase in ER over a temperature range from 0°C to 30°C . The average temperature sensitivity of GPP amounted to 0.54 (Fig. 4; Table 3), predicting a 9.7-fold increase in GPP over a temperature range from 0°C to 30°C . Thus, as predicted from the metabolic theory, ER increased more with temperature than did GPP. Consequently, according to Eqs. 3, 4, the activation energy of the ER/GPP ratio was expected to average 0.08 eV. This corresponds to a predicted 1.4-fold increase in the ratio over a temperature range from 0°C to 30°C . Although close to the theoretically predicted value, the actual estimated average activation energy of 0.13 eV for the ER/GPP ratio was not significant (Fig. 5a; Table 3).

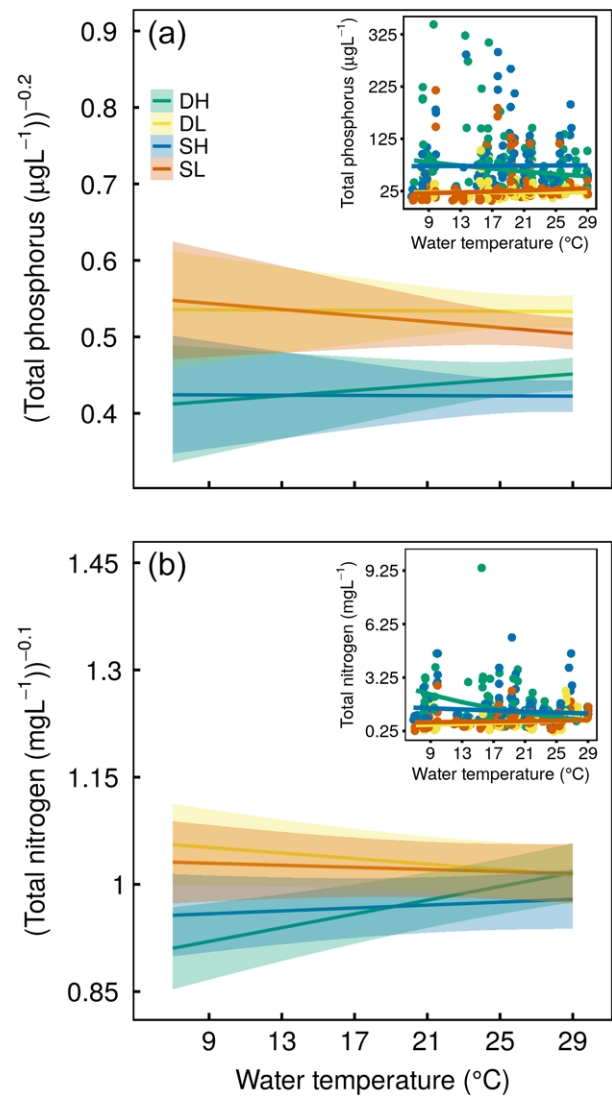


Fig. 2. Covariation of nutrients with water temperature. Covariation of monthly (a) TP and (b) TN levels with water temperature by treatment. Main images show treatment-specific least-square means over the temperature gradient with 95% confidence intervals at the scale of the transformed variable. The insets depict TP and TN at original scale with treatment-specific average TP or TN concentrations as estimated by mixed effects regression (Supporting Information S3 Table 1). DH, deep high nutrient; SH, shallow high nutrient; DL, deep low nutrient; and SL, shallow low nutrient treatment.

However, due to lower absolute ER/GPP ratios in eutrophic compared with mesotrophic systems, the mesotrophic mesocosms had, on average, a 10% lower metabolic-driven carbon sequestration capacity than the eutrophic mesocosms over a temperature range from 0°C to 30°C .

The effect of covariates on metabolic rates

The average temperature sensitivity for daylight length-corrected GPP had an estimated average activation energy of

Table 2. Results from minimal linear mixed effect regressions. The effects of inverse scaled temperature (invT), depth (*D*) and nutrients (*N*), as well as their interactions, were tested on: GPP per day, ER per day, primary production per daylight hour (GPP_{dl}), and the ratio between ecosystem respiration and gross primary production (ER/GPP). Effect size is given as regression coefficients from standardized predictors (shallow = -0.5, deep = 0.5, low = -0.5, high = 0.5). The first R^2 value refers to the marginal R^2 (variance explained by fixed factors) and the second to the conditional R^2 (variance explained by fixed and random factors).

Response	Predictor	Effect size	SE	T-value	p value	R^2
ln (GPP)	Int	11.34	0.14	77.99	< 0.01	0.50, 0.8
	invT	-0.91	0.16	-3.29	0.02	
	D	-0.55	0.03	-9.93	< 0.01	
	N	0.58	0.03	10.52	< 0.01	
ln (ER)	Int	11.37	0.32	34.99	< 0.01	0.33, 0.88
	invT	-1.05	0.24	-2.54	0.06	
	D	-0.58	0.03	-9.37	< 0.01	
	N	0.48	0.03	7.91	< 0.01	
ln (GPP _{dl})	Int	8.71	0.18	46.68	< 0.01	0.34, 0.78
	invT	-0.53	0.15	-2.03	0.10	
	D	-0.54	0.03	-9.74	< 0.01	
	N	0.58	0.03	10.49	< 0.01	
ln (ER/GPP)	Int	-0.01	0.14	-0.41	0.71	0.04, 0.60
	invT	-0.22	0.10	-1.27	0.27	
	D	-0.01	0.02	-0.20	0.85	
	N	-0.09	0.02	-1.99	0.05	

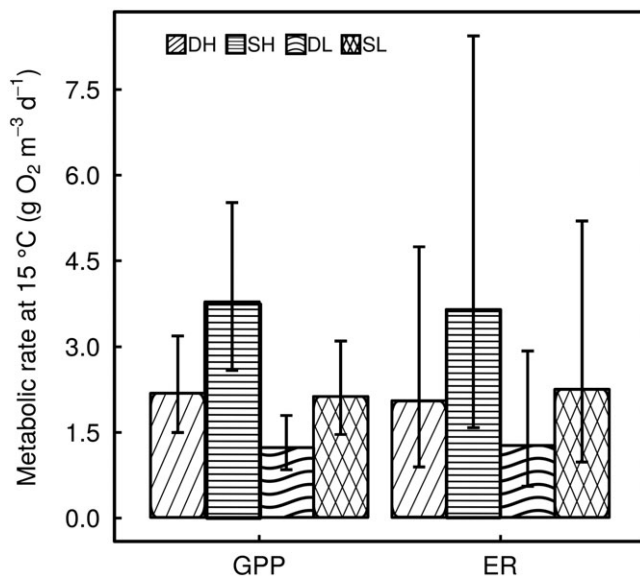


Fig. 3. Treatment-wise metabolic rates at 15°C as estimated by mixed effects regression. Values were back transformed to original scale, depicting the geometric mean (Table 3). Error bars represent the 95% confidence interval of the geometric mean. DH, deep high nutrient; SH, shallow high nutrient; DL, deep low nutrient; and SL, shallow low nutrient treatment.

0.31 eV, and was thus close to the canonical temperature dependence of photosynthesis. However, it was not significant at the 0.05% level (Table 2).

Results from semi-partial Spearman correlations confirmed the importance of temperature for metabolic rates independent of light-related factors (Table 4). As expected, however, light-related factors were also significantly correlated with GPP, except in shallow mesotrophic systems. Significant correlations between GPP and Chl *a* or PVI were observed in systems in which these drivers were highest, i.e., in the eutrophic and mesotrophic shallow mesocosms (Supporting Information S3 Fig. 2, Table 4). In addition to temperature, ER was strongly correlated with GPP.

Temperature-specific switch from autotrophy to heterotrophy (Hypothesis 4)

In the mesotrophic mesocosms, based on Eq. 5 and average values from the mixed effects regression for GPP and ER (Table 3), the switch from autotrophy to heterotrophy generally occurred at lower temperatures (12°C and 10°C) than in the eutrophic mesocosms (21°C and 19°C) (Fig. 5b). This is in line with our prediction. In contrast, light regime and mixing depth had only a minor impact on the switch point. This is confirmed by a significant nutrient effect ($p = 0.05$), but an insignificant depth effect ($p = 0.85$) for the ER/GPP ratio (Fig. 5a; Table 2).

Discussion

It is anticipated that climate change will affect shallow lake metabolism and thereby the ability of such lakes to sequester

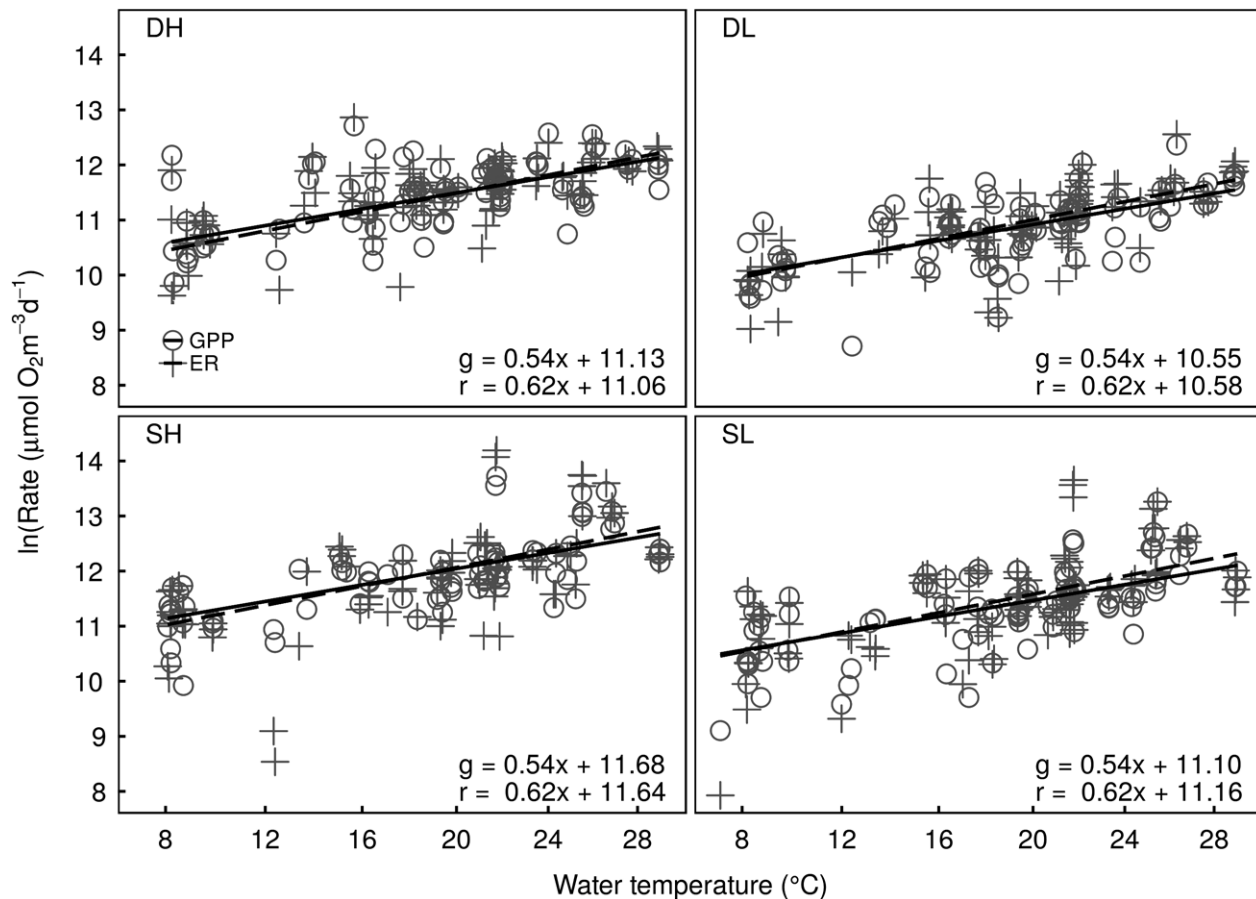


Fig. 4. Arrhenius plot of GPP and ER for each treatment (DH, deep high nutrient; SH, shallow high nutrient; DL, deep low nutrient; and SL, shallow low nutrient). The plot is based on monthly measurements from July to November along a temperature gradient from Sweden to Greece. The solid line is the estimated average GPP; the dotted line is the average ER as estimated by mixed effects regression. Note that the actual units of the x-axis of the Arrhenius plot are $1/k$ ($1/T_c - 1/T$) in units of electron volts and a reference temperature, T_c , of 15°C ; for easier interpretation, corresponding temperatures in degrees Celsius are depicted.

carbon due to direct and indirect impacts on major drivers such as temperature, nutrients, water level, and light conditions (Tranvik et al. 2009; Nickus et al. 2010; Jeppesen et al. 2015). We confirmed the existence of a positive relationship between nutrient concentrations, light availability, temperature, and metabolic rates in shallow lakes.

The observed apparent differential temperature sensitivity between GPP and ER adds support to the anticipated shift (Cole et al. 2000; Staehr and Sand-Jensen 2006; Yvon-Durocher et al. 2010a,b) toward an increasing degree of heterotrophy in shallow lake ecosystems with increasing temperatures. Since the observed activation energy for ER was higher than for GPP, ER increased more than production, leading to a predicted increase in ER/GPP over the tested temperature gradient. The average temperature sensitivity of the ER/GPP ratio itself was not significant, perhaps due to the inherent variance of both the GPP and the ER estimates. Nonetheless, the estimated average activation energy of 0.13 eV is in accordance with the predicted values of 0.08 eV based on Eq. 4 (Fig. 5b).

The established apparent average temperature sensitivities of the metabolic rates of 0.62 eV and 0.31 eV for ER and GPP per daylight hour, respectively, match well with predictions for the physiological temperature dependence for respiration (0.6 eV) and photosynthesis (0.3 eV) predicted by the metabolic theory (Allen et al. 2005). With a value of 0.54 eV , the observed activation energy of GPP per day exceeds the predicted physiological temperature dependence, but closely conforms to findings from other aquatic environments: $0.50 \pm 0.18\text{ eV}$ (Wilken et al. 2013); $0.54 \pm 0.24\text{ eV}$ (Demars et al. 2011); and 0.45 eV (95% CI $0.38\text{--}0.53$) (Yvon-Durocher et al. 2010b). Most algae and cyanobacteria have carbon-concentration mechanisms (CCMs) to prevent the oxygenase activity of Rubisco, particularly under low pCO_2 and high-alkalinity conditions (Raven et al. 2011; Falkowski and Raven 2007; Demars et al. 2016). CCMs are assumed to be the cause of the systematic higher activation energy for GPP found in freshwater systems compared with the activation energy derived for terrestrial C3 plants (Demars et al. 2015, 2016). The alkalinity in our systems was at intermediate levels on

Table 3. Slope (activation energy), intercept (average metabolic rate at 15°C), and temperature at which the systems switch from autotrophy to heterotrophy. Slope and intercept values are derived from minimal mixed effect models, i.e., models from which all insignificant terms are removed, but which contain at least the inverse scaled temperature and the main effects of the depth and nutrient treatment (Table 2). 95% confidence intervals are given in brackets. Confidence intervals for activation energies were computed based on likelihood profiles (“confint.merMod” function of the “lme4” package). Treatment-specific confidence intervals for the intercepts were computed based on *t*-statistics with degrees of freedom determined by the Kenward-Rogers method (“lsmeans” function of the “lsmeans” package). DH, deep high nutrient; SH, shallow high nutrient; DL, deep low nutrient; and SL, shallow low nutrient treatment.

		GPP	ER	GPP _{dl}	ER/GPP
activation Energy (eV)	DH	0.54 (0.9–0.2)	0.62 (1.14–0.11)	0.31 (0.65 to –0.11)	0.13 (0.36 to –0.08)
	SH				
	DL				
	SL				
Intercept at 15°C ln[$\mu\text{mol O}_2 \text{ m}^{-3} \text{ d}^{-1}$]	DH	11.13 (10.78–11.47)	11.06 (10.30–11.83)	8.60 (8.15–9.06)	–0.11 (–0.47 to 0.26)
	SH	11.68 (11.33–12.02)	11.64 (10.87–12.41)	9.14 (8.69–9.60)	–0.10 (–0.46 to 0.27)
	DL	10.55 (10.20–10.90)	10.58 (9.81–11.35)	8.03 (7.57–8.48)	–0.02 (–0.38 to 0.35)
	SL	11.10 (10.75–11.45)	11.16 (10.39–11.92)	8.57 (8.11–9.03)	–0.01 (–0.38 to 0.35)
Switch point temperature (°C)	DH		21	—	21
	SH		19	—	21
	DL		12	—	16
	SL		10	—	16

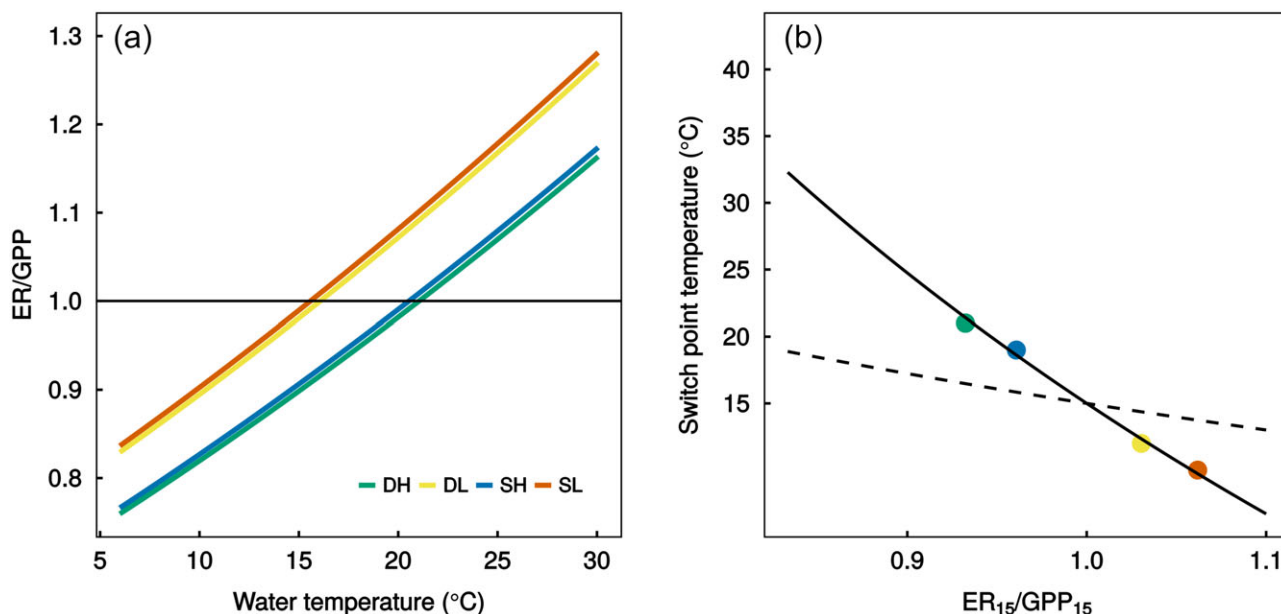


Fig. 5. Water temperature-dependent switch from net autotrophy to net heterotrophy. **(a)** Average treatment-specific change in ER/GPP ratio over the temperature gradient as estimated by mixed effect model (Table 3). **(b)** Theoretically predicted switch point temperatures from autotrophy to heterotrophy depending on the ER/GPP ratio at a reference temperature of 15°C (Eq. 5). The solid line depicts the switch point temperature for activation energies of 0.54 eV and 0.62 eV for GPP and ER, respectively. The dashed line represents the relation at an activation energy of 0.31 eV for GPP, as suggested by the MTE and established as the average apparent activation energy for daylight length-corrected primary production. Superimposed are the treatment-wise average switch point temperatures as established by mixed effects regression (Table 3). DH, deep high nutrient; SH, shallow high nutrient; DL, deep low nutrient; and SL, shallow low nutrient treatment.

average (mean $1363 \pm 27 \text{ mol L}^{-1} \text{ eq HCl}$). pCO_2 levels, estimated from midday alkalinity and daily average pH (Trolle et al. 2012), indicate the potential of low pCO_2 episodes

(mean $\text{epCO}_2 \approx 0.55 \pm 0.07$ times atmospheric pressure), making the active operation of CCMs likely. However, in our systems, high-positive correlations between daylight length

Table 4. Bootstrapped semi-partial spearman correlation coefficient r over all treatments (all) and treatment-specific (S, shallow; D, deep; H, high nutrient; L, low nutrient) for the three criterion variables GPP, ER, and ER/GPP and the following predictor variables: Inverse-scaled temperature (invT), Chl a , PVI, LP_{eff}, MAL, daylight length (DayL), ER/GPP ratio, GPP, and ER. Only r values ≥ 0.10 are reported, “*” denotes values where the 95% confidence interval did not include zero, “–” denotes cells of variables not used as predictors for the particular variable.

		invT	Chl a	PVI	LP _{eff}	MAL	DayL	GPP
GPP	All	–0.23*	0.33*		–0.12*	0.24*		–
	DH	–0.22	0.28*		–0.15*	0.16	0.15	–
	SH	–0.40*	0.23*	0.12			0.25*	–
	DL	–0.41*			–0.18*	0.13		–
	SL	–0.28*		0.27*				–
ER	All	–0.19*			–	–	–	0.52*
	DH	–0.27*			–	–	–	0.43*
	SH	–0.19*	0.1	0.14*	–	–	–	0.32*
	DL	–0.28*		0.12	–	–	–	0.38*
	SL	–0.19*			–	–	–	0.38*
ER/GPP	All	–0.23*					–0.10*	–
	DH	–0.16	–0.12			–0.14		–
	SH	–0.20*			–0.12			–
	DL	–0.29*				–0.16	–0.11	–
	SL	–0.25*			–0.16			–

and temperature serve as a reasonable explanation for the higher-than-expected activation energy, as daylight length-corrected estimates led to the physiologically predicted temperature sensitivity of 0.31 eV. Interestingly, regions with seasonal temperature fluctuations exhibit a natural correlation between daylight length and temperature, possibly mitigating the expected shift toward heterotrophy.

The expected temperature at which a system switches from autotrophy to heterotrophy can be modeled in the framework of MTE according to Eq. 5. The model suggests that the temperature threshold at which a system switches from net autotrophic to net heterotrophic depends on the extent of the differential temperature sensitivity between GPP and ER (E_p and E_r , respectively) and on the log ratio between GPP and ER at a reference temperature, T_c (here, 15°C). This temperature threshold turned out to be affected by trophic state (Fig. 5a): higher nutrient availability in the eutrophic mesocosms led not only to significantly higher GPP and ER, but also to significantly lower ER to GPP ratios (0.9 [DH] and 0.91 [SH]) than under mesotrophic conditions (0.98 [DL] and 0.99 [SL]). This apparently small difference was, however, large enough to cause an average temperature threshold increase of approximately 5°C (based on ER/GPP ratio). Thus, under the predicted warming scenarios of 1.5–5°C by 2100 (Rogelj et al. 2012; Stocker et al. 2014), high-nutrient systems are likely to have a lower risk of becoming net heterotrophic than systems with lower nutrient concentrations (Fig. 5b; Table 3). The direct effect of water depth on the ER/GPP ratio was not significant, and the effect of depth on the threshold temperature was low, indicating that a reduced water level is of minor importance

for the switch from autotrophy to heterotrophy in these generally shallow systems.

In our experiment, the confirmation of the MTE was strong when aggregating data from all countries and seasons, while at the same time, temperature sensitivity exhibited a relatively high idiosyncrasy between countries (Supporting Information S4 Table 2). This is in line with findings from other studies, where single systems tend to deviate from the MTE predictions (De Castro and Gaedke 2008; Davidson et al. 2015), while larger-scale studies are often in good agreement with the predictions (López-Urrutia et al. 2006; Yvon-Durocher et al. 2012). Potential mechanisms behind this variation include acclimatization and adaptation processes, which are hypothesized to induce reduced temperature sensitivity with increasing average temperature (Atkin and Tjoelker 2003; Hikosaka et al. 2006; Hartley et al. 2008; Angilletta 2009; Smith and Dukes 2012). In this study, we found no evidence for a systematic change in activation energy with average temperature (Supporting Information S4 Table 2), which is in line with Perkins et al. (2012), who reported consistent Q10 temperature coefficient values for ER regardless of the thermal history or community composition of biofilms, as well as with a global survey of activation energies based on satellite data by Kraemer et al. (2016).

Furthermore, contrary to our expectations, we observed no significant interactions between the temperature sensitivity of both GPP and ER and nutrient levels, or depth. We can only speculate about the underlying mechanisms. Perhaps the missing depth-temperature interaction reflects light adaptation, rendering photosynthesis primarily dependent on the

maximum photosynthetic rate. The lack of TP-temperature interaction indicates that either TP affinity was not a function of temperature, or that shifts in community composition in the mesotrophic mesocosms toward species with higher phosphate affinity prevented limitation of photosynthesis by phosphorus (de Senerpont Domis et al. 2014). However, lack of sensitivity to depth and nutrients may also reflect the relatively modest variations in these experimental variables.

Therefore, a better understanding of the factors leading to deviations from MTE-predicted temperature sensitivity remains an important area of research.

A decline in water level, as already reported and further anticipated within the context of global warming for lakes in the Mediterranean region (Coops et al. 2003; Beklioglu et al. 2006, 2007; Jeppesen et al. 2015), affects mixing depth and light availability. We found a significantly lower GPP and ER in deep than in shallow mesocosms (Table 3). The difference in production levels was most likely generated by the influence of depth on the light availability, while impacts on gas exchange due to a lower surface-to-volume ratio were most likely negligible since all mesocosms were fully mixed. Light saturation for photosynthesis is specific to each algal species and ranges from around 60–100 $\mu\text{mol m}^{-2} \text{s}^{-1}$ (Lampert and Sommer 1999). This confines deep mesocosms to the lower end of the range, and makes them more prone to being light-limited, while the shallow mesocosms are close to, or above, the upper end of the range (Supporting Information S3 Table 1), and thus most likely light-saturated. Additionally, only in the eutrophic deep systems was the sediment layer generally below the euphotic zone; thus, only these mesocosms had a considerably shorter average LP_{eff} compared with all other treatments (Supporting Information S3 Table 1). Therefore, a reduction in water level considerably improves light availability, and might allow benthic primary production where it was not possible before.

The linear mixed effect regression approach is an optimal method for analyzing our data as long as we can reasonably assume a generic temperature sensitivity of metabolic rates or random variation in temperature sensitivity due to interactions with factors randomly varying between countries (see Supporting Information S8). Since the between-country comparison of systematic changes in temperature sensitivity with average temperature indicated no systematic change (see Supporting Information S4), there is solid justification for the approach used in this study. Furthermore, this approach would be sensitive to interactions between average temperature sensitivity and nutrients, or between average temperature sensitivity and water level. However, the use of this approach also implies that we must analyze temperature sensitivity, as it responds to seasonal temperature changes, as opposed to controlled experimental temperature manipulation. The temperature response of ecosystem level metabolic rates based on seasonal data captures the apparent temperature sensitivity toward relatively short-termed temperature changes and

cannot replace a true experimental test of the effect of global warming (therefore, we use “apparent” temperature sensitivity). This is a limitation, but the response to seasonal temperature changes is of scientific interest, since seasonal temperature changes are the dimension along which the property of temperature sensitivity takes effect in ecosystems. Like all experimental approaches, mesocosm experiments come with inherent abstractions from the natural complexity, as well as their own challenges, which restrict a direct generalization of results to natural systems. In our experimental design, the constant mixing by aquarium pumps creates ideal constant mixing conditions, which prevents the natural variability in mixing intensity, including micro- and short-term stratification events. Mixing-induced fluctuation in light conditions has been shown to influence phytoplankton growth rates (Shatwell et al. 2012, Köhler et al. 2018), and stratification influences the availability of nutrients and oxygen (Wilhelm and Adrian 2008). In turn, phytoplankton growth impacts water transparency and thus water temperature and the mixing regime (Shatwell et al. 2016). However, differential warming of our mesocosms due to differences in water transparency was prevented, since water temperature in the mesocosms was mainly determined by the surrounding lake. Another well-known general problem in mesocosm studies is periphyton growth on the walls of the enclosures, forming in part a micro-environment. There is limited knowledge about the influence of periphyton on nutrient cycling and metabolic rates in the open water column, which prevents quantification (Wetzel 2001; Petersen 2009). Furthermore, our experimental design may have influenced the proportion of GPP to ER, as we included sediment, which contained foreign organic matter that may have enhanced ER at higher temperatures and, thus, the ratio. While this may potentially affect the absolute values (if not in equilibrium with the current conditions in the mesocosm) of thresholds regarding the shift to heterotrophy, it does not affect the observed direction of changes and the overall conclusions. However, the absolute thresholds should be interpreted with caution.

Research indicates that shallow lakes play an important role in local and global carbon cycling, as they are the most numerous type of lake in the world (Tranvik et al. 2009; Cael et al. 2017). Given that a differential temperature sensitivity of ER and GPP poses a potential feedback mechanism to atmospheric CO_2 levels in a warming scenario, understanding the metabolic processes of shallow lake ecosystems, and how they will be affected by a changing climate, is not only of basic but also of applied ecological interest. The results of this study confirmed and quantified the varying apparent temperature sensitivity of GPP and ER and showed that trophic state is important for the question of how much warming a shallow lake system can tolerate before it switches from net autotrophy to net heterotrophy.

We linked our experimental findings with the framework of the MTE and tested theoretically derived predictions on our

data. In line with earlier studies, we found good agreement between theory and practice, which affirmed the potential of the MTE also in the context of shallow lakes. Furthermore, we found that the balance between ER and GPP depends not only on the energy supply, as in the MTE, but also on the availability of nitrogen and phosphorus. Thus, we conclude that quantitative inclusion of these nutrients in the MTE, as suggested for instance by Allen and Gillooly (2009), Anderson-Teixeira and Vitousek (2012), and Davidson et al. (2012), could greatly add to its predictive power for shallow lakes.

References

- Allen, A. P., J. F. Gillooly, and J. H. Brown. 2005. Linking the global carbon cycle to individual metabolism. *Funct. Ecol.* **19**: 202–213. doi:[10.1111/j.1365-2435.2005.00952.x](https://doi.org/10.1111/j.1365-2435.2005.00952.x)
- Allen, A. P., and J. F. Gillooly. 2009. Towards an integration of ecological stoichiometry and the metabolic theory of ecology to better understand nutrient cycling. *Ecol. Lett.* **12**: 369–384. doi:[10.1111/j.1461-0248.2009.01302.x](https://doi.org/10.1111/j.1461-0248.2009.01302.x)
- Anderson-Teixeira, K. J., and P. M. Vitousek. 2012. Ecosystems, p. 99–111. *In* R. M. Sibly, J. H. Brown, and A. Kodric-Brown [eds.], *Metabolic ecology*. Wiley-Blackwell. doi:[10.1002/9781119968535](https://doi.org/10.1002/9781119968535)
- Andersson, E., and S. Sobek. 2006. Comparison of a mass balance and an ecosystem model approach when evaluating the carbon cycling in a lake ecosystem. *Ambio* **35**: 476–483. doi:[10.1579/0044-7447\(2006\)35\[476:COAMBA\]2.0.CO;2](https://doi.org/10.1579/0044-7447(2006)35[476:COAMBA]2.0.CO;2)
- Angilletta, M. J. J. 2009. *Thermal adaptation - a theoretical and empirical synthesis*. Oxford Univ. Press.
- Atkin, O. K., and M. G. Tjoelker. 2003. Thermal acclimation and the dynamic response of plant respiration to temperature. *Trends Plant Sci.* **8**: 343–351. doi:[10.1016/S1360-1385\(03\)00136-5](https://doi.org/10.1016/S1360-1385(03)00136-5)
- Balmer, M. B., and J. A. Downing. 2011. Carbon dioxide concentrations in eutrophic lakes: Undersaturation implies atmospheric uptake. *Inland Waters* **1**: 125–132. doi:[10.5268/IW-1.2.366](https://doi.org/10.5268/IW-1.2.366)
- Bartoń, K. 2015. MuMIn: Multi-model inference. R package version 1.13.4. Available from <http://cran.r-project.org/package=MuMIn>. Access date 2015-02-24
- Bates, D., M. Maechler, B. Bolker, and S. Walker. 2014. lme4: Linear mixed-effects models using Eigen and S4. R package version 1.1-7. Available from <http://cran.r-project.org/package=lme4>. Access date 2014-07-19
- Beklioglu, M., G. Altınayar, and C. T. Tan. 2006. Water level control over submerged macrophyte development in five Mediterranean Turkey. *Arch. Hydrobiol.* **166**: 535–556. doi:[10.1127/0003-9136/2006/0166-0535](https://doi.org/10.1127/0003-9136/2006/0166-0535)
- Beklioglu, M., S. Romo, I. Kagalou, X. Quintana, and E. Bécars. 2007. State of the art in the functioning of shallow Mediterranean Lakes: Workshop conclusion. *Hydrobiologia* **196**: 317–326. doi:[10.1007/s10750-007-0577-x](https://doi.org/10.1007/s10750-007-0577-x)
- Berggren, M., H. Laudon, A. Jonsson, and M. Jansson. 2010. Nutrient constraints on metabolism affect the temperature regulation of aquatic bacterial growth efficiency. *Microb. Ecol.* **60**: 894–902. doi:[10.1007/s00248-010-9751-1](https://doi.org/10.1007/s00248-010-9751-1)
- Bernacchi, C. J., E. L. Singaas, C. Pimentel, A. R. Portis Jr., and S. P. Long. 2001. Improved temperature response functions for models of Rubisco-limited photosynthesis. *Plant Cell Environ.* **24**: 253–259. doi:[10.1111/j.1365-3040.2001.00668.x](https://doi.org/10.1111/j.1365-3040.2001.00668.x)
- Brothers, S. M., and others. 2013. A regime shift from macrophyte to phytoplankton dominance enhances carbon burial in a shallow, eutrophic lake. *Ecosphere* **4**: 1–17. doi:[10.1890/ES13-00247.1](https://doi.org/10.1890/ES13-00247.1)
- Brown, J. H., J. F. Gillooly, A. P. Allen, V. M. Savage, and G. B. West. 2004. Toward a metabolic theory of ecology. *Ecology* **85**: 1771–1789. doi:[10.1890/03-9000](https://doi.org/10.1890/03-9000)
- Cael, B. B., A. J. Heathcoate, and D. A. Seekell. 2017. The volume and mean depth of Earth's lakes. *Geophys. Res. Lett.* **44**: 209–218. doi:[10.1002/2016GL071378](https://doi.org/10.1002/2016GL071378)
- Canty, A., and B. Ripley. 2015. boot: Bootstrap R (S-Plus) functions. R package version 1.3-15. Available from <http://cran.r-project.org/package=boot>. Access date 2015-02-10
- Cole, J. J., M. L. Pace, S. R. Carpenter, and J. F. Kitchell. 2000. Persistence of net heterotrophy in lakes during nutrient addition and food web manipulations. *Limnol. Oceanogr.* **45**: 1718–1730. doi:[10.4319/lo.2000.45.8.1718](https://doi.org/10.4319/lo.2000.45.8.1718)
- Cole, J. J., and others. 2007. Plumbing the global carbon cycle: Integrating inland waters into the terrestrial carbon budget. *Ecosystems* **10**: 172–185. doi:[10.1007/s10021-006-9013-8](https://doi.org/10.1007/s10021-006-9013-8)
- Coloso, J. J., J. J. Cole, and M. L. Pace. 2011. Difficulty in discerning drivers of lake ecosystem metabolism with high frequency data. *Ecosystems* **14**: 935–948. doi:[10.1007/s10021-011-9455-5](https://doi.org/10.1007/s10021-011-9455-5)
- Coops, H., M. Beklioglu, and T. L. Crisman. 2003. The role of water-level fluctuations in shallow lake ecosystems – workshop conclusions. *Hydrobiologia* **506**: 23–27. doi:[10.1023/B:HYDR.0000008595.14393.77](https://doi.org/10.1023/B:HYDR.0000008595.14393.77)
- Cross, W., J. Hood, J. Benstead, A. Huryn, and D. Nelson. 2015. Interactions between temperature and nutrients across levels of ecological organization. *Glob. Chang. Biol.* **21**: 1025–1040. doi:[10.1111/gcb.12809](https://doi.org/10.1111/gcb.12809)
- Davidson, E. A., S. Samanta, S. C. Samantha, and K. Savage. 2012. The Dual Arrhenius and Michaelis-Menten kinetics model for decomposition of soil organic matter at hourly to seasonal time scales. *Glob. Chang. Biol.* **18**: 371–384. doi:[10.1111/j.1365-2486.2011.02546.x](https://doi.org/10.1111/j.1365-2486.2011.02546.x)
- Davidson, T. A., J. Audet, J.-C. Svenning, T. L. Lauridsen, M. Søndergaard, F. Landkildehus, S. E. Larsen, and E. Jeppesen. 2015. Eutrophication effects on greenhouse gas fluxes from shallow-lake mesocosms override those of climate warming. *Glob. Chang. Biol.* **21**: 4449–4463. doi:[10.1111/gcb.13062](https://doi.org/10.1111/gcb.13062)
- De Castro, F., and U. Gaedke. 2008. The metabolism of lake plankton does not support the metabolic theory of ecology. *Oikos* **117**: 1218–1226. doi:[10.1111/j.0030-1299.2008.16547.x](https://doi.org/10.1111/j.0030-1299.2008.16547.x)
- De Matos, M. P., A. C. Borges, A. T. de Matos, E. F. da Silva, and M. A. Martinez. 2014. Effect of time-temperature

- binomial in obtaining biochemical oxygen demand of different wastewaters. *Eng. Agric.* **34**: 332–340. doi:[10.1590/S0100-69162014000200014](https://doi.org/10.1590/S0100-69162014000200014)
- De Rosario-Martinez, H. 2015. phia: Post-hoc interaction analysis. R package version 0.2-0. Available from <http://cran.r-project.org/package=phia>. Access date 2015-02-25
- de Senerpont Domis, L. N., D. B. van de Waal, N. R. Helmsing, E. van Donk, and W. M. Mooij. 2014. Community stoichiometry in a changing world: Combined effects of warming and eutrophication on phytoplankton dynamics. *Ecology* **95**: 1485–1495. doi:[10.1890/13-1251.1](https://doi.org/10.1890/13-1251.1)
- del Giorgio, P. A., and R. H. Peters. 1994. Patterns in planktonic P:R ratios in lakes: Influence of lake trophic and dissolved organic carbon. *Limnol. Oceanogr.* **39**: 772–787. doi:[10.4319/lo.1994.39.4.0772](https://doi.org/10.4319/lo.1994.39.4.0772)
- Demars, B. O. L., and others. 2011. Temperature and the metabolic balance of streams. *Freshw. Biol.* **56**: 1106–1121. doi:[10.1111/j.1365-2427.2010.02554.x](https://doi.org/10.1111/j.1365-2427.2010.02554.x)
- Demars, B. O. L., J. Thompson, and J. R. Manson. 2015. Stream metabolism and the open diel oxygen method: Principles, practice, and perspectives. *Limnol. Oceanogr.: Methods* **13**: 356–374. doi:[10.1002/lom3.10030](https://doi.org/10.1002/lom3.10030)
- Demars, B. O. L., G. M. Gislason, J. S. Ólafsson, J. R. Manson, N. Friberg, J. M. Hood, J. J. D. Thompson, and T. E. Freitag. 2016. Impact of warming on CO₂ emission from streams countered by aquatic photosynthesis. *Nat. Geosci.* **9**: 758–761. doi:[10.1038/ngeo2807](https://doi.org/10.1038/ngeo2807)
- Duarte, C. M., S. Agustí, and D. Vaqué. 2004. Controls on planktonic metabolism in the Bay of Blanes, northwestern Mediterranean littoral. *Limnol. Oceanogr.* **49**: 2162–2170. doi:[10.4319/lo.2004.49.6.2162](https://doi.org/10.4319/lo.2004.49.6.2162)
- Enquist, B. J., E. P. Economo, T. E. Huxman, A. P. Allen, D. D. Ignace, and J. F. Gillooly. 2003. Scaling metabolism from organisms to ecosystems. *Nature* **423**: 639–642. doi:[10.1038/nature01671](https://doi.org/10.1038/nature01671)
- Erlandsen, M., and N. Thyseen. 1983. Modelling the community oxygen production in lowland streams dominated by submerged macrophytes, p. 855–860. *In* W. K. Lauenroth and G. V. Skogerboe [eds.], *Analysis of ecological systems: State-of-the art in ecological modelling*, v. 5. Elsevier. doi:[10.1016/B978-0-444-42179-1.50096-1](https://doi.org/10.1016/B978-0-444-42179-1.50096-1)
- Falkowski, J. A., and A. Raven. 2007. *Aquatic photosynthesis*, 2nd ed. Princeton Univ. Press.
- Gelman, A. 2008. Scaling regression inputs by dividing by two standard deviations. *Stat. Med.* **27**: 2865–2873. doi:[10.1002/sim.3107](https://doi.org/10.1002/sim.3107)
- Gillooly, J. F., J. H. Brown, G. B. West, V. M. Savage, and E. L. Charnov. 2001. Effects of size and temperature on metabolic rate. *Science* **293**: 2248–2251. doi:[10.1126/science.1061967](https://doi.org/10.1126/science.1061967)
- Hanson, P. C., D. L. Bade, S. R. Carpenter, and T. K. Kratz. 2003. Lake metabolism: Relationships with dissolved organic carbon and phosphorus. *Limnol. Oceanogr.* **48**: 1112–1119. doi:[10.4319/lo.2003.48.3.1112](https://doi.org/10.4319/lo.2003.48.3.1112)
- Hartley, I. P., D. W. Hopkins, M. H. Garnett, M. Sommerkorn, and P. A. Wookey. 2008. Soil microbial respiration in arctic soil does not acclimate to temperature. *Ecol. Lett.* **11**: 1092–1100. doi:[10.1111/j.1461-0248.2008.01223.x](https://doi.org/10.1111/j.1461-0248.2008.01223.x)
- Hikosaka, K., K. Ishikawa, A. Borjigidai, O. Muller, and Y. Onoda. 2006. Temperature acclimation of photosynthesis: Mechanisms involved in the changes in temperature dependence of photosynthetic rate. *J. Exp. Bot.* **57**: 291–302. doi:[10.1093/jxb/erj049](https://doi.org/10.1093/jxb/erj049)
- Jeppesen, E., and others. 2012. Biomanipulation as a restoration tool to combat eutrophication: Recent advances and future challenges. *Adv. Ecol. Res.* **47**: 411–488. doi:[10.1016/B978-0-12-398315-2.00006-5](https://doi.org/10.1016/B978-0-12-398315-2.00006-5)
- Jeppesen, E., and others. 2015. Ecological impacts of global warming and water abstraction on lakes and reservoirs due to changes in water level and related changes in salinity. *Hydrobiologia* **750**: 201–227. doi:[10.1007/s10750-014-2169-x](https://doi.org/10.1007/s10750-014-2169-x)
- Kim, S. 2012. ppcor: Partial and semi-partial (Part) correlation. R package version 1.0. Available from <http://cran.r-project.org/package=ppcor>. Access date 2012-10-29
- Kirk, J. T. O. 2010. *Light and photosynthesis in aquatic ecosystems*, 3rd ed. Cambridge Univ. Press. doi:[10.1017/CBO9781139168212](https://doi.org/10.1017/CBO9781139168212)
- Köhler, J., L. Wang, A. Guislan, and T. Shatwell. 2018. Influence of vertical mixing on light-dependency of phytoplankton growth. *Limnol. Oceanogr.* **63**: 1156–1167. doi:[10.1002/lno.10761](https://doi.org/10.1002/lno.10761)
- Kosten, S., F. Roland, D. M. L. Da Motta Marques, E. H. van Nes, N. Mazzeo, L. D. L. Sternberg, M. Scheffer, and J. J. Cole. 2010. Climate-dependent CO₂ emissions from lakes. *Global Biogeochem. Cycles* **24**: 1–7. doi:[10.1029/2009GB003618](https://doi.org/10.1029/2009GB003618)
- Kraemer, B. M., and others. 2016. Global patterns in lake ecosystem responses to warming based on the temperature dependence of metabolism. *Glob. Chang. Biol.* **56**: 1447–1455. doi:[10.1111/gcb.13459](https://doi.org/10.1111/gcb.13459)
- Kuznetsova, A., P. B. Brockhoff, and R. H. Bojesen. 2014. lmerTest: Tests in linear mixed effects models. R package version 2.0-20. Available from <http://cran.r-project.org/package=lmerTest>. Access date 2014-11-22
- Laas, A., P. Nöges, T. Kõiv, and T. Nöges. 2012. High-frequency metabolism study in a large and shallow temperate lake reveals seasonal switching between net autotrophy and net heterotrophy. *Hydrobiologia* **694**: 57–74. doi:[10.1007/s10750-012-1131-z](https://doi.org/10.1007/s10750-012-1131-z)
- Lampert, W., and U. Sommer. 1999. *Limnoökologie*, 2nd ed. Georg Thieme Verlag.
- Landkildehus, F., and others. 2014. Climate change effects on shallow lakes: Design and preliminary results of a cross-European climate gradient mesocosm experiment. *Est. J. Ecol.* **63**: 71–89. doi:[10.3176/eco.2014.2.02](https://doi.org/10.3176/eco.2014.2.02)
- Lenth, R. V., and M. Hervé. 2015. Least-squares means. R package version 2.16. Available from <http://cran.r-project.org/package=lsmeans>. Access date 2015-03-14

- Liboriussen, L., T. L. Lauridsen, M. Søndergaard, F. Landkildehus, M. Søndergaard, S. E. Larsen, and E. Jeppesen. 2011. Effects of warming and nutrients on sediment community respiration in shallow lakes: An outdoor mesocosm experiment. *Freshw. Biol.* **56**: 437–447. doi:[10.1111/j.1365-2427.2010.02510.x](https://doi.org/10.1111/j.1365-2427.2010.02510.x)
- López-Urrutia, Á., E. San Martín, R. P. Harris, and X. Irigoien. 2006. Scaling the metabolic balance of the oceans. *Proc. Natl. Acad. Sci. USA* **103**: 8739–8744. doi:[10.1073/pnas.0601137103](https://doi.org/10.1073/pnas.0601137103)
- McFeeters, B. J., and P. C. Frost. 2011. Temperature and the effects of elemental food quality on *Daphnia*. *Freshw. Biol.* **56**: 1447–1455. doi:[10.1111/j.1365-2427.2011.02586.x](https://doi.org/10.1111/j.1365-2427.2011.02586.x)
- Moss, B. 2010. Climate change, nutrient pollution and the bargain of Dr Faustus. *Freshw. Biol.* **55**: 175–187. doi:[10.1111/j.1365-2427.2009.02381.x](https://doi.org/10.1111/j.1365-2427.2009.02381.x)
- Nickus, U., and others. 2010. Direct impacts of climate change on freshwater ecosystems, p. 38–64. *In* M. Kernan, R. W. Battarbee, and B. Moss [eds.], *Climate change impacts on freshwater ecosystems*. Wiley-Blackwell. doi:[10.1002/9781444327397](https://doi.org/10.1002/9781444327397)
- Pacheco, F., F. Roland and J. A. Downing. 2014. Eutrophication reverses whole-lake carbon budgets. *Inland Waters* **4**: 41–48. doi:[10.5268/IW-4.1.614](https://doi.org/10.5268/IW-4.1.614)
- Perkins, D. M., G. Yvon-Durocher, B. O. L. Demars, J. Reiss, D. E. Pichler, N. Friberg, M. Trimmer, and G. Woodward. 2012. Consistent temperature dependence of respiration across ecosystems contrasting in thermal history. *Glob. Chang. Biol.* **18**: 1300–1311. doi:[10.1111/j.1365-2486.2011.02597.x](https://doi.org/10.1111/j.1365-2486.2011.02597.x)
- Petersen, J. 2009. *Enclosed experimental ecosystems and scale: Tools for understanding and managing coastal ecosystems*. Springer. doi:[10.1007/978-0-387-76767-3](https://doi.org/10.1007/978-0-387-76767-3)
- R Core Team. 2015. R: A language and environment for statistical computing. Available from <http://www.R-project.org/>. Access date 2015-05-01
- Raven, J. A., M. Giordano, J. Beardall, and S. C. Maberly. 2011. Algal and aquatic plant carbon concentration mechanisms in relation to environmental change. *Photosyn. Res.* **109**: 281–296. doi:[10.1007/s11120-011-9632-6](https://doi.org/10.1007/s11120-011-9632-6)
- Ripley, B., B. Venables, D. M. Bates, K. Hornik, A. Gebhardt, and D. Firth. 2015. MASS: Modern applied statistics with S. R package version 7.3–40. Available from <http://cran.r-project.org/package=MASS>. Access date 2015-03-21
- Rogelj, J., M. Meinshausen, and R. Knutti. 2012. Global warming under old and new scenarios using IPCC climate sensitivity range estimates. *Nat. Clim. Chang.* **2**: 248–253. doi:[10.1038/nclimate1385](https://doi.org/10.1038/nclimate1385)
- Sadro, S., J. M. Melack, and S. MacIntyre. 2011. Spatial and temporal variability in the ecosystem metabolism of a high-elevation lake: Integrating benthic and pelagic habitats. *Ecosystems* **14**: 1123–1140. doi:[10.1007/s10021-011-9471-5](https://doi.org/10.1007/s10021-011-9471-5)
- Shatwell, T., A. Nicklisch, and J. Köhler. 2012. Temperature and photoperiod effects on phytoplankton growing under simulated mixed layer light fluctuations. *Limnol. Oceanogr.* **57**: 541–553. doi:[10.4319/lo.2012.57.2.0541](https://doi.org/10.4319/lo.2012.57.2.0541)
- Shatwell, T., R. Adrian, and G. Kirillin. 2016. Planktonic events may cause polymictic-dimictic regime shifts in temperate lakes. *Sci. Rep.* **6**: 24361. doi:[10.1038/srep24361](https://doi.org/10.1038/srep24361)
- Smith, N. G., and J. S. Dukes. 2012. Plant respiration and photosynthesis in global-scale models: Incorporating acclimation to temperature and CO₂. *Glob. Chang. Biol.* **19**: 45–63. doi:[10.1111/j.1365-2486.2012.02797.x](https://doi.org/10.1111/j.1365-2486.2012.02797.x)
- Solomon, C. T., and others. 2013. Ecosystem respiration: Drivers of daily variability and background respiration in lakes around the globe. *Limnol. Oceanogr.* **58**: 849–866. doi:[10.4319/lo.2013.58.3.0849](https://doi.org/10.4319/lo.2013.58.3.0849)
- Staehr, P. A., and K. Sand-Jensen. 2006. Seasonal changes in temperature and nutrient control of photosynthesis, respiration and growth of natural phytoplankton communities. *Freshw. Biol.* **51**: 249–262. doi:[10.1111/j.1365-2427.2005.01490.x](https://doi.org/10.1111/j.1365-2427.2005.01490.x)
- Staehr, P. A., and K. Sand-Jensen. 2007. Temporal dynamics and regulation of lake metabolism. *Limnol. Oceanogr.* **52**: 108–120. doi:[10.4319/lo.2007.52.1.0108](https://doi.org/10.4319/lo.2007.52.1.0108)
- Staehr, P. A., K. Sand-Jensen, A. L. Raun, B. Nilsson, and J. Kidmose. 2010. Drivers of metabolism and net heterotrophy in contrasting lakes. *Limnol. Oceanogr.* **55**: 817–830. doi:[10.4319/lo.2009.55.2.0817](https://doi.org/10.4319/lo.2009.55.2.0817)
- Stocker, T. F., Q. Dahe, and G.-K. Plattner. 2014. Technical Summary, p. 33–116. *In* *Climate Change 2013: The physical science basis. Contribution of working group I to the fifth assessment report of the Intergovernmental Panel on Climate Change*. Cambridge Univ. Press. doi:[10.1017/CBO9781107415324.005](https://doi.org/10.1017/CBO9781107415324.005)
- Streeter, H. W., and E. B. Phelps. 1925. A study of the natural purification of the Ohio River. *Public Health Bulletin* 146. U.S. Public Health Service. URI: <http://udspace.udel.edu/handle/19716/1590>
- Tranvik, L. J., and others. 2009. Lakes and reservoirs as regulators of carbon cycling and climate. *Limnol. Oceanogr.* **54**: 2298–2314. doi:[10.4319/lo.2009.54.6_part_2.2298](https://doi.org/10.4319/lo.2009.54.6_part_2.2298)
- Trolle, D., P. A. Staehr, T. A. Davidson, R. Bjerring, T. L. Lauridsen, M. Søndergaard, and E. Jeppesen. 2012. Seasonal dynamics of CO₂ flux across the surface of shallow temperate lakes. *Ecosystems* **15**: 336–347. doi:[10.1007/s10021-011-9513-z](https://doi.org/10.1007/s10021-011-9513-z)
- Welter, J. R., P. B. Jonathan, W. F. Cross, J. M. Hood, A. D. Huryn, P. W. Johnson, and T. J. Williamson. 2015. Does N₂ fixation amplify the temperature dependence of ecosystem metabolism? *Ecology* **93**: 603–610. doi:[10.1890/14-1667.1](https://doi.org/10.1890/14-1667.1)
- Wetzel, R. G. 2001. *Limnology: Lake and river ecosystems*, 3rd ed. Academic Press.
- Weyhenmeyer, G. A., S. Kosten, M. B. Wallin, L. J. Tranvik, E. Jeppesen, and R. Fabio. 2015. Significant fraction of CO₂ emissions from boreal lakes derived from hydrologic inorganic carbon inputs. *Nat. Geosci.* **8**: 933–936. doi:[10.1038/ngeo2582](https://doi.org/10.1038/ngeo2582)
- Wilhelm, S., and R. Adrian. 2008. Impact of summer warming on the thermal characteristics of a polymictic lake and

- consequences for oxygen, nutrients and phytoplankton. *Freshw. Biol.* **53**: 226–237. doi:[10.1111/j.1365-2427.2007.01887.x](https://doi.org/10.1111/j.1365-2427.2007.01887.x)
- Wilken, S., J. Huisman, S. Naus-Wiezer, and E. van Donk. 2013. Mixotrophic organisms become more heterotrophic with rising temperature. *Ecol. Lett.* **16**: 225–233. doi:[10.1111/ele.12033](https://doi.org/10.1111/ele.12033)
- Wykoff, D. D., J. P. Davies, A. Melis, and A. R. Grossman. 1998. The regulation of photosynthetic electron transport during nutrient deprivation in *Chlamydomonas reinhardtii*. *Plant Physiol.* **117**: 129–139. doi:[10.1104/pp.117.1.129](https://doi.org/10.1104/pp.117.1.129)
- Yvon-Durocher, G., A. P. Allen, J. M. Montoya, M. Trimmer, and G. Woodward. 2010a. The temperature dependence of the carbon cycle in aquatic ecosystems, p. 267–313. In G. Woodward [ed.], *Advances in ecological research*, v. 43. Elsevier. doi:[10.1016/B978-0-12-385005-8.00007-1](https://doi.org/10.1016/B978-0-12-385005-8.00007-1)
- Yvon-Durocher, G., J. I. Jones, M. Trimmer, G. Woodward, and J. M. Montoya. 2010b. Warming alters the metabolic balance of ecosystems. *Philos. Trans. R. Soc. Biol. Sci.* **365**: 2117–2126. doi:[10.1098/rstb.2010.0038](https://doi.org/10.1098/rstb.2010.0038)
- Yvon-Durocher, G., and others. 2012. Reconciling the temperature dependence of respiration across timescales and ecosystem types. *Nature* **487**: 472–476. doi:[10.1038/nature11205](https://doi.org/10.1038/nature11205)

Acknowledgments

We thank the technical staff at the various experimental sites for their support. We thank Alena S. Gesell, Deniz Özkundakci, Jan-Hendrik Schleimer, Silke Schmidt, Torsten Seltmann, and Tom Shatwell for their helpful discussions during the preparation of this manuscript. We thank Anne Mette Poulsen, Adam Wilkins, and Michael Thayne for their valuable editing of the manuscript. We are also grateful to reviewers for their valuable comments on the manuscript. This study was supported by FP-7 REFRESH (Adaptive strategies to Mitigate the Impacts of Climate Change on European Freshwater Ecosystems, Contract No. 244121) and the MARS project (Managing Aquatic ecosystems and water Resources under multiple Stress), funded under the 7th EU Framework Programme, Theme 6 (Environment including Climate Change), Contract No. 603378 (<http://www.mars-project.eu>), TUBITAK-ÇAYDAG (projects No. 105Y332 and 110Y125), the Middle East Technical University (METU)-BAP program of Turkey. EJ was further supported by AU Centre for Water Technology and AİÇ was also supported by TUBITAK (project 296 Nos. 105Y332 and 110Y125).

Conflict of Interest

None declared.

Submitted 17 January 2018

Revised 22 June 2018

Accepted 19 September 2018

Associate editor: Marguerite Xenopoulos